 doi:10.20944/preprints202005.0278.v1

FLOW PATTERN AND PRESSURE DROP FOR OIL-WATER FLOWS IN AND AROUND 180^{O} BENDS

Paul Onubi Ayegba.[1,2], Lawrence C. Edomwonyi-Otu[2,3*], Abdulkareem Abubakar[2], Nurudeen Yusuf[4],

[1]Department of Mechanical Engineering University of California Berkeley, 94720 CA, USA.
[2]Department of Chemical Engineering Ahmadu Bello University, 810212 Zaria, Nigeria.
[3]Department of Chemical and Petroleum Engineering, Delta State University, 330106 Abraka, Nigeria.
[4]Department of Chemical and Petroleum Engineering, Bayero University, 700231 Kano, Nigeria.

*Corresponding Author: uceclce@ucl.ac.uk

ABSTRACT

Pressure drop and flow pattern of oil-water flows were investigated in a 19 mm ID clear polyvinyl chloride pipe consisting of U-bend with radius of curvature of 100 mm. The range for oil and water superficial velocities tested were $0.04 \leq U_{so} \leq 0.950\, m/s$ and $0.13 \leq U_{sw} \leq 1.10\, m/s$ respectively. Measurements were carried out under different flow conditions in a test section that consisted of four different parts: upstream of the bend, at the bend and at two redeveloping flow locations after the bend. The result indicated that the bend had limited influence on downstream flow patterns. However, the shear forces imposed by the bend caused some shift flow pattern transition and bubble characteristics in the redeveloping flow section after the bend relative to develop flow before the bend. Generally, pressure gradient at all the test sections increased with both oil fraction and water superficial velocity and there was a sharp change of pressure gradient profile during phase inversion. The transition point where phase inversion occurred was always within the range of $0.4 \leq U_{sw} \leq 0.54\, m/s$. Pressure losses differed at the various test sections and the difference was strongly linked to the superficial velocity of the phases and the flow pattern. At high mixture velocity, pressure losses at the redeveloping section after the bend were higher than that at the bend and that for fully developed flows. At low mixture velocity, pressure losses at the bend are higher than in the straight sections. Pressure drop generally decreased with level of flow development downstream of the bend.

Key Words: U-bend; oil-water flow; flow pattern; pressure losses; flow redevelopment.

NOMENCLATURE

DP	Pressure drop
DP_L	Pressure gradient
R	Radius of curvature
d	Pipe diameter
f	Friction factor
ST	Stratified
DC	Dual continuous
Do/w/w	Dispersed oil in water and water
Do/w	Dispersed oil in water

Preprints (www.preprints.org) | NOT PEER-REVIEWED | Posted: 16 May 2020 doi:10.20944/preprints202005.0278.v1

Dw/o	Dispersed water in oil
Subscripts	
SO	Superficial Oil
SW	Superficial Water
M	Mixture

1 INTRODUCTION

Co-current flow of oil and water in pipeline is common in chemical, process and petroleum industry operations [1]. Data on flow development/redevelopment, pressure drop, flow pattern, phase mixing and interfacial characteristics are essential for optimal design and operation in the industries as well as for modelling [2]–[4]. In petroleum exploration and transport, connate water or injected water from enhanced oil recovery operations flow along with oil. Also, in the transport of high viscosity oils, water injection into the annulus of pipelines has been used as a means of reducing friction losses and by extension reduce pumping power requirements [5]–[11].

The behavior of the fluid flow in bends is complex due to the action of centrifugal forces on the mixture along with the under-developed flow profile in bends [12]–[14]. Wall and interfacial frictions in oil-water two flows contribute the most to pressure gradient in developed flows in straight horizontal smooth pipes [15]–[18]. In curved pipes and for undeveloped flows, additional losses result from secondary flows and form drag consequent upon the effect of centrifugal forces and flow redistribution. The contribution of secondary flows to pressure drops, relative to wall and interface frictions, is significant at moderate flowrates in turbulent flow regime. Therefore, when secondary flow contribution is significant, the pressure drops in bends is markedly higher than that in straight pipes of comparable length. The difference generally increases with curvature ratio and decreases with the length of the bend. At higher flowrates, the effect of turbulence and interfacial tension dominates and pressure drops in bends and straight pipes may assume asymptotic convergence. Pressure drops for redeveloping oil-water flows after bends result from the combination of wall friction, interfacial friction and phase redistribution (form drag). While pressure drop due to wall and interfacial friction are primarily functions of fluid rheological properties and flow rate, the contribution of flow redistribution is a strong function the level of flow disturbance generated at the bend (or other fitting). The flow disturbances downstream of bends with small radius of curvature are relatively small and therefore wall friction dominates. The higher the interfacial tension, the higher its contribution to pressure drops in liquid-liquid flows [16], [18]. Another parameter which has affects oil-water flow characteristics is the pipe diameter. Al-Wahaibi et al., (2014) studied the influence of pipe diameter on flow patterns and pressure gradient for oil-water flows in horizontal straight pipes of 19 mm and 25.4 mm IDs. The region of dual continuous and dispersed oil in water increased with pipe diameter. Whereas, the region of stratified, bubbly and annular flows decreased as pipe diameter increased. They also reported an increase in pressure gradient with mixture velocity. Regardless of the flow geometry and flow

Preprints (www.preprints.org) | NOT PEER-REVIEWED | Posted: 16 May 2020 doi:10.20944/preprints202005.0278.v1

disturbances, pressure drops for oil-water flows depend on the flow pattern and more so on the continuity of the phases [19], [20].

Few investigations have been conducted on the co-current flow of oil and water in U-bends with the view of characterising the flow patterns and pressure drops associated with such flows [21]–[23]. With regards to the effect of U-bends on post-bend flow pattern characteristics, it has been reported that it is strongly influenced by fluid properties such as oil viscosity. Sharma et al., (2011b) observed flow patterns in U-bend as well at 120 x ID (hydrodynamically developed flow) before and after a U-bend for the flow of low-viscosity-oil (kerosene)-water in horizontal; upward and downward flow directions. The viscosity and density of kerosene used were $\mu_o = 1.2\, mPa.s$ and $\rho_o = 787\ kg/m^3$ respectively and the bend curvature ratio ($2R/d$) was 16.67. They categorised the observed flow regimes into stratified flow, plug flow, kerosene dispersed, water dispersed and core annular flow. Besides film inversion (consequent upon centrifugal forces in the bend), flow patterns before and after the bend were largely similar in all three flow directions. The implication of this is that the bend and the direction of flow had little or no influence on flow patterns downstream of the bend. This is not surprising considering that flow pattern observation was done at locations before and after the bend where flows are fully developed. Interestingly, in the horizontal flow direction, flow patterns in all three sections (U-bend, before the U-bend and after the U-bend) were very similar. Equally interesting is that core annular flow was only reported in the return bend for upward and downward flow directions. In a separate investigation (with same experimental setup) using high-viscosity-oil (lube), Sharma et al. (2011a), reported that the bend as well the direction of flow had significant influence on the downstream flow patterns. The viscosity and density of lube used are $\mu_o = 220\, mPa.s$ and $\rho_o = 960\ kg/m^3$ respectively. Not only was the flow pattern before and after the bend different for a given flow direction, but it varied from one flow direction to the other. This is may be associated with the significant difference in viscosity of kerosene and lube oil and the resulting difference in interfacial stress between kerosene-water and lube-water. Also, flow development is a function of Reynolds number which in turn depends on fluid viscosity. It should also be stated that they reported a predominance of core annular flow in their lube-water experiments and an additional flow pattern classified as droplet flow which was absent in the kerosene-water experiments of Sharma et al. (2011b). The predominance of core annular flow is signature characteristics of high-viscosity oil-water flows and similar behaviour is reported for straight pipe flows [24]. Pietrzak (2014) in their study of oil-water flow in horizontal U-bends categorised flow patterns in terms of the dominant continuous phase (oil dominant, W/O or water dominant, O/W). Their flow pattern characterisation was however limited to the U-bend and did not extend to effects of the bend on downstream flow patterns. One of the goals of this work is to examine the effect of the bend on flow pattern and flow pattern transition in the downstream redeveloping section immediately downstream of the bend. In summary, flow patterns associated with oil-water flows in and around U-bend are schematically presented in Figure *1*.

Preprints (www.preprints.org) | NOT PEER-REVIEWED | Posted: 16 May 2020 doi:10.20944/preprints202005.0278.v1

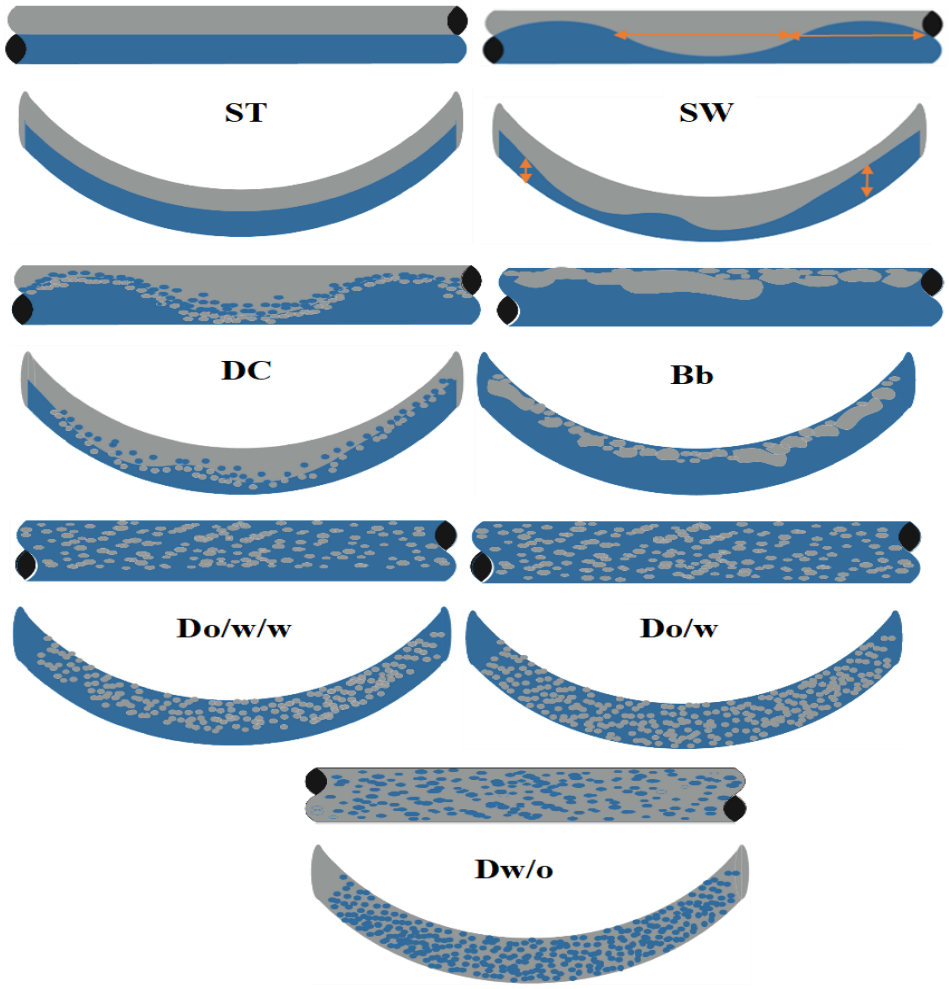

Figure 1: Sketches of flow patterns in and around U-bend.

A few experimental and modelling studies have been done to study the pressure drop of oil-water two-phase flows in U-bends [22], [23], [25]. Analogous to straight pipe flows, pressure drop for oil-water two-phase flows in U-bends increases with flowrate of either of the phases and more so with the more viscous phase [22], [23], [25]. In the kerosene-water experiments of Sharma et al. (2011b), they reported higher pressure drop in the bend relative to upstream and downstream straight pipe sections where flows were hydrodynamically developed. This is expected, considering the additional bend loss due to the action of centrifugal forces on the flow at the bend along with the fact that pressure measurements before and after the bend were done for hydrodynamically developed flows. They also reported similar pressure drops across the U-bend in horizontal, upward and downward flow directions. This suggests that gravitational component of pressure gradient in upward and downward flows is small. Sharma et al. (2011a) in their investigation of high-viscosity oil-water flow in U-bend, also recorded similar pressure drop both before and after the return bend for all three flow directions in spite of the difference in flow patterns. Again, this can be linked to the fact that pressure drop measurements were done at developed flow sections before and after the U-bend. Research on the characteristics (pressure drop and flow pattern) of redeveloping flows after the bend is lacking and this research seeks to bridge this gap.

Preprints (www.preprints.org) | NOT PEER-REVIEWED | Posted: 16 May 2020 doi:10.20944/preprints202005.0278.v1

2 MATERIALS AND METHOD

2.1 Materials

Table 1 gives a summary of the properties of the test fluids used in this study.

Table 1: Test fluid properties at 22^o C

Test fluids	Density (kg/m^3)	Viscosity (mPa.s)	Surface tension (mN/m)	Oil-Water interfacial tension (mN/m)
Tap water	998.2	1.0016	72.5	40.94
White mineral oil	835	10.55	29.2	

2.2 Experimental flow loop and procedures

The experimental rig used for this study was a two-phase flow loop assembled by the authors for oil-water flow experiments at the Richmond Field Station of University of California Berkeley (Figure *2*). The setup included the holding, regulating and test sections. The holding section consisted of 3 conical-bottom inductor tanks each of 60-gallon capacity. The tanks were for oil, water and oil-water separation. The regulating section had two 1-hp centrifugal *CF* pumps, connecting pipes, valves and two Coriolis mass flow meters (CMFS050M, 0-70 lbmin^{-1}). Two flow meters were used for measuring the flowrates of oil and water. They also provided values for density, temperature among other fluid properties. The test section was made up of two parallel 19-mm ID clear PVC pipes joined by a U-bend with radius of 100 mm. The test section, divided into four parts, had five differential pressure transducers (four Yokogawa 0-35 mmHg differential pressure (DP) transducers (model EJX 110A) and one Foxboro 0-850 mmHg DP transducer (model IDP10). One Yokogawa DP transducers was connected across a pair of pressure ports situated at 63.5 and 177.8 cm (114.3 cm apart) before the U-bend and used for measuring differential pressure of fully developed flow before the bend. A flow development length of 4.8 m was provided before the high-pressure port of this transducer. Another Yokogawa DP transducer was connected across the U-bend on a pair of pressure ports that were 31.1 cm apart. A third Yokogawa DP transducer was connected across a pair of pressure ports situated 14.0 and 128.3 cm (114.3 cm apart) downstream of the bend and used for differential pressure measurement immediately after the bend (i.e. redeveloping station 1). The last Yokogawa DP transducer was connected across a pair of pressure ports located at 63.5 and 177.8 cm (114.3 cm apart) downstream of the bend and used for taking measurement of pressure drop at a second section (i.e. station 2) further downstream of the bend (redeveloping section 2). The Foxboro DP transducer was connected across a pair of pressure ports situated at 12.7 cm before the bend and 434.3 cm after the bend and used for taking measurement of the combined pressure drop due to bend and redeveloping section. This transducer served the purpose of validating results of the other transducers. All pressure ports were situated along the base of the test pipe and the DP transducers were calibrated before use. Finally, each differential pressure or pressure drop measured was divided by the distance between the ports over which it was measured to obtain pressure gradient.

Three Basler Ace USB high-speed cameras were situated at 30.5 cm before -, mid-way across - and 30.5 cm after - the bend for flow pattern identification. The cameras before and after the bend were installed at 0^o to the horizontal plane and perpendicular to the flow. The camera at

Preprints (www.preprints.org) | NOT PEER-REVIEWED | Posted: 16 May 2020 doi:10.20944/preprints202005.0278.v1

the bend was installed at 35^{o} to the horizontal and perpendicular to the flow. The choice of angle was informed by the changes in the angle of the interface with changes in the superficial velocities of the phases. At lower flowrates when buoyancy effect dominated, the interface was almost horizontal (with water occupying the bottom section and oil the top). However, as relative velocity increased and centrifugal forces became significant, the interface inclined at an angle to the vertical and even became almost vertical at high relative velocities. In this case, water occupied the outer curve while oil occupied the inner side. All three flow pattern-identifying locations were provided with rectangular viewing boxes filled with pure glycerine to minimize optical distortion due to pipe curvatures. Simultaneous image capturing was carried out with all three cameras at a framerate of 57 fps and the exposure time was varied to suit the mixture flowrates. Flow pattern identification was carried out by careful examination of over 1000 closeup images combined with experimental notes and continuity of phases. All five differential transducers and the two Coriolis flow meters were connected to a computer for data acquisition via LabVIEW interface. For voltage measurements, 500 ohms ($\pm$5%) standard resistors were connected across the data acquisition terminals. However, to establish a base line and for reliability, direct voltage measurements were carried out across the terminals. The high-speed cameras were connected to three USB-3.0 ports on the computer.

Test measurements were carried out by varying the oil flowrate for a given water flowrate. The range of flowrates for water and oil were 0.13 – 1.1 m/s and 0.04 – 0.95 m/s respectively. The LabVIEW VI was setup to take simultaneous measurements from all the DP transducers, the two Coriolis flow meters and all three cameras. A minimum of 300 pressure and superficial velocity data sets were collected for each measurement run and the runs were repeated at least three times at every measurement condition under consideration. $\pm$2.6% maximum measurement error was recorded for differential pressure.

Preprints (www.preprints.org) | NOT PEER-REVIEWED | Posted: 16 May 2020 doi:10.20944/preprints202005.0278.v1

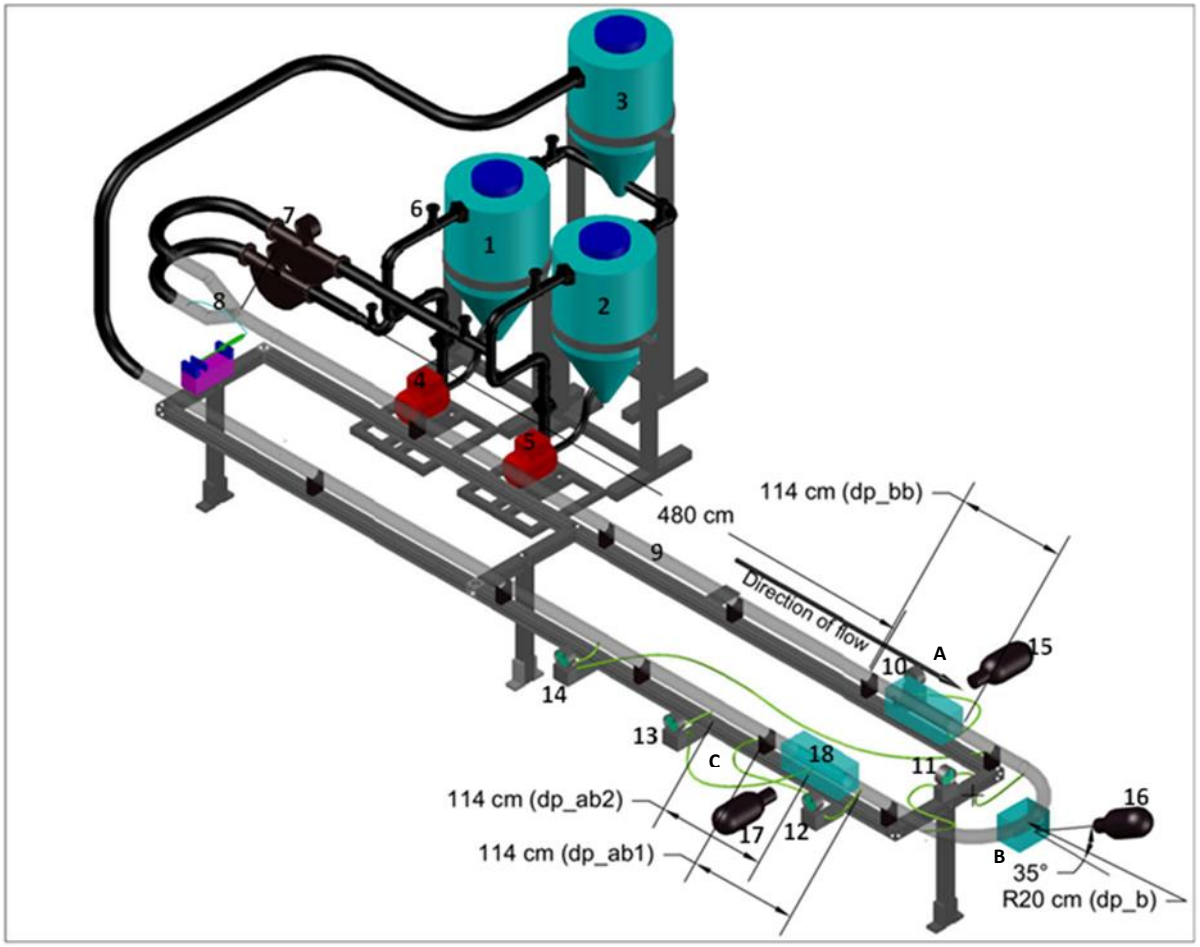

Figure 2: Sketch of the experimental flow rig, 1. Water storage tank 2. Oil storage tank 3. Separation tank 4. Water CF pump 5. Oil CF pump 6. Gate valves 7. Coriolis mass flow meters 8. Y-junction 9. Clear PVC test section 10. DP transducer (before bend) 11. DP transducer (across bend) 12. DP transducer (after bend 1) 13. DP transducer (after bend 2) 14. DP transducer (bend + redeveloping flow section) 15. Camera (before bend) 16. Camera (bend) 17. Camera (after bend) 18. Rectangular view boxes.

3 RESULTS AND DISCUSSION

3.1 Flow patterns in and around return bend

Six flow regimes were identified over the measurement range and in all the test sections. These were stratified flow (ST), dual continuous or three-layer flow (DC), Bubbly/Plug flow (Bb), dispersed oil in water and water layer (Do/w/w), dispersed oil in water (Do/w) and dispersed water in oil (Dw/o).

Stratified flow (ST): At very low oil and water superficial velocities, buoyancy forces dominated in all test sections and the oil and water phases occupied the top and bottom sections of the pipe respectively, separated by a smooth horizontal interface (Figure 3a). With small increase in superficial velocity of either or both phases, long-wavelength asymmetric waves began to emerge at the interface. The crests of the waves were generally sharper than the troughs, which had longer wavelengths (Figure 3b). As the effect of centrifugal forces became significant relative to buoyancy and inertia forces, the stratified flow characteristic at the bend

Preprints (www.preprints.org) | NOT PEER-REVIEWED | Posted: 16 May 2020 doi:10.20944/preprints202005.0278.v1

showed a marked difference from those in the straight sections of the flow. The interfacial height at the entry of the bend was lower than that at the exit (Figure 3b) and the interface was inclined to the vertical. The inclination was such that the interfacial height at the outer bend became higher than that at the inner bend. With further increase in the flowrate of water, the inclination of the interface increased and a maximum inclination of 75° to the horizontal plane was observed.

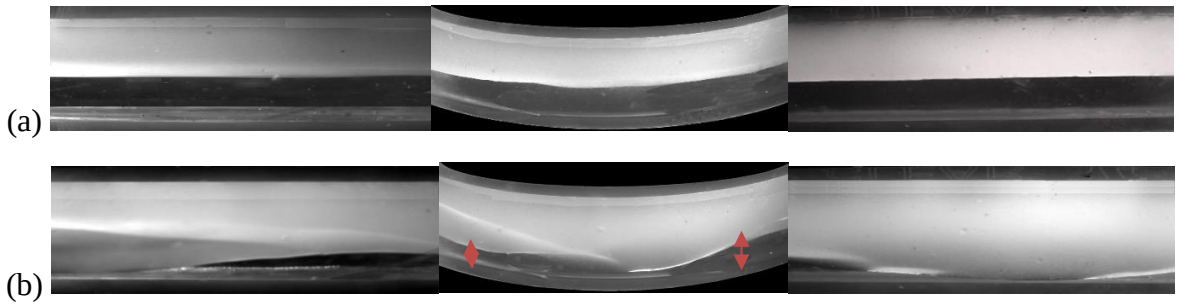

Figure 3: Camera images of stratified flow. (a) $U_{SO} = 0.12\, ms^{-1}$, $U_{SW} = 0.13 ms^{-1}$; (b) $U_{SO} = 0.24 ms^{-1}$, $U_{SW} = 0.13 ms^{-1}$. From left to right: fully developed flow before the bend, at the bend and redeveloping flow after the bend

Dual continuous (DC)/Three-layer flow: As the relative velocity of the phases was increased further, critical interfacial shear was reached and droplets began to form near the wavy interface (Figure 4). Droplets of water was seen in the oil phase close to the interface and vice versa. The flow was still largely separated with clear oil and water phases at the top and bottom pipe sections respectively. At higher mixture velocities, the wavy structure disappears and a layer of mixed oil and water bubbles form around the interface. This type of DC flow was described as three-layer flow by Al-Yaari et al., (2012) (Figure 5a). The DC or three-layer flow pattern characteristic in the straight sections were pretty similar. However, close inspection revealed that the bubble diameters for the redeveloping flow after the bend appeared smaller while the bubbles became more elongated. This was due to the shear forces impacted by the bend on the flow. Meanwhile, some unique features were identified at the bend. Firstly, the interface was inclined with the inclination as high as 75° to the horizontal at higher mixture velocities just like in the case stratified flow. Secondly, the bubbles occupied a thin layer that was inclined to the horizontal and thirdly, a thin intermittent oil film began to form at the outer wall whose thickness and duration scaled with oil superficial velocity (Figure 5b).

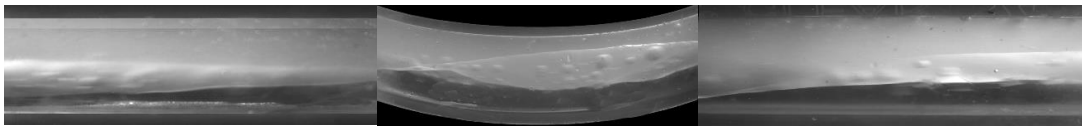

Figure 4: Camera images of DC flow at $U_{SO} = 0.1236 ms^{-1}$ and $U_{SW} = 0.27 ms^{-1}$. From left to right: fully developed flow before the bend, at the bend and redeveloping flow after the bend

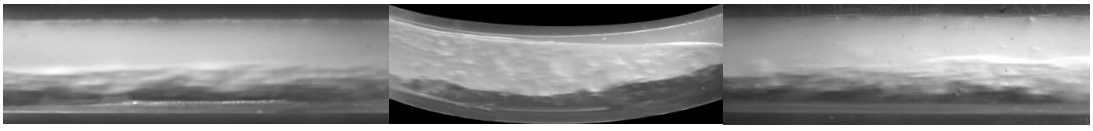

Preprints (www.preprints.org) | NOT PEER-REVIEWED | Posted: 16 May 2020 doi:10.20944/preprints202005.0278.v1

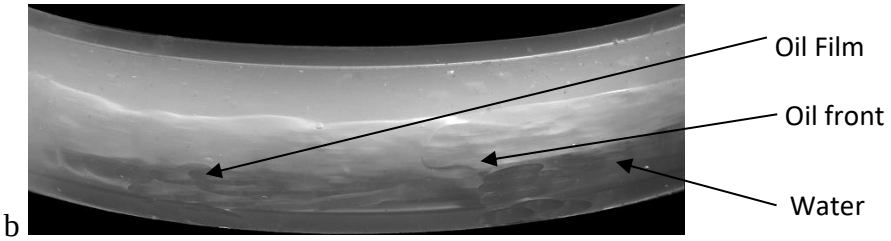

b

Figure 5: a. Camera images of three-layer flow at $U_{SO} = 0.48ms^{-1}$ and $U_{SW} = 0.27ms^{-1}$. From left to right: fully developed flow before the bend, at the bend and redeveloping flow after the bend. b. Camera image of tree-layer flow in U-bend with intermittent oil film at the outer wall.

Bubbly/Plug flow: This occurred at moderate water flowrate and low oil superficial velocity. Elongated bubbles/plugs flowed at the top end of the pipe whereas water formed the continuous phase. Bubble diameter or plug length were similar to or longer than the pipe diameter. The bubbles/plugs were more closely packed in the hydrodynamically developed straight flow upstream of the bend and less so at the bend and after the bend. This was due to shear forces exacted by the bend on the bubbles (Figure 6).

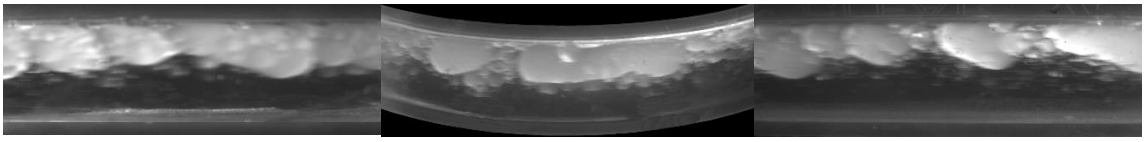

Figure 6: Camera images of bubbly/plug flow at $U_{SO} = 0.12ms^{-1}$and $U_{SW} = 0.4ms^{-1}$. From left to right: fully developed flow before the bend, at the bend and redeveloping flow after the bend

Dispersed oil in water and water (Do/w/w): At high water superficial velocity and low oil superficial velocity, oil was dispersed in water. Do/w/w flow regime occurred in the range of $0.4 \leq U_{SW} \leq 1.07\, ms^{-1}$, $U_{SO} \leq 0.24ms^{-1}$. In this range of superficial velocities, the buoyancy effect was still significant relative to inertia effect and a clear water layer flowed at the bottom section of the conduit. The thickness of this water layer decreased with increase in oil fraction (Figure 7).

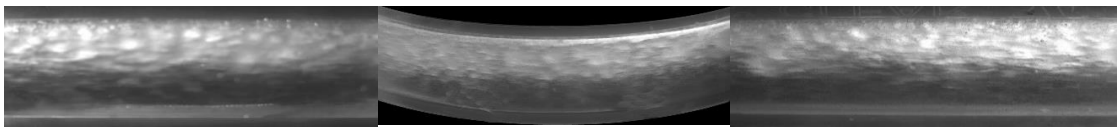

Figure 7: Camera images of dispersed oil in water & water at $U_{SO} = 0.12ms^{-1}$ and $U_{SW} = 0.54ms^{-1}$. From left to right: fully developed flow before the bend, at the bend and redeveloping flow after the bend

Dispersed oil in water (Do/w): At high mixture velocities in the water dominant regime, the oil phase was fully dispersed in the water phase (Figure 8). In this flow regime, the inertia force was dominant over gravitational forces and the oil was dispersed all through the pipe cross section. It is important to state that with increasing oil superficial velocity, the transition from Do/w/w to Do/w did not always occur at the same oil superficial velocities in the hydrodynamically developed flow before bend and the redeveloping flow after the bend. The transition in the case of redeveloping flows sometimes occurred at higher superficial velocities

Preprints (www.preprints.org) | NOT PEER-REVIEWED | Posted: 16 May 2020 doi:10.20944/preprints202005.0278.v1

of the oil phase. This can be attributed to the fact that the centrifugal forces at the bend, imposed phase separation on the mixture and this phase separation was carried on to the section after the bend thereby creating a thin layer of clear water later at the bottom tube section. The difference was not always obvious due to limited image resolution. At the bend, Do/w flow pattern always seemed to have a very thin water layer at the outer wall of the bend but oil droplets were intermittently suspended in this water layer.

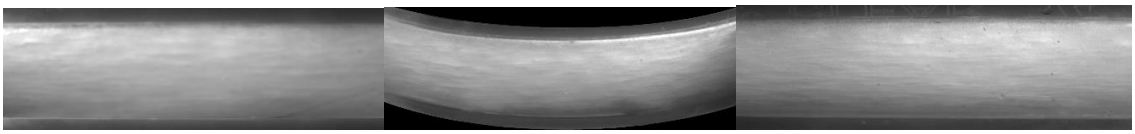

Figure 8: Camera images of dispersed oil in water flow at $U_{SO} = 0.84ms^{-1}$ and $U_{SW} = 1.07ms^{-1}$. From left to right: fully developed flow before the bend, at the bend and redeveloping flow after the bend

Dispersed water in oil (Dw/o): At high oil superficial velocities and low water superficial velocity, elliptical-shaped water droplets were dispersed throughout the oil continuous phase (Figure 9).

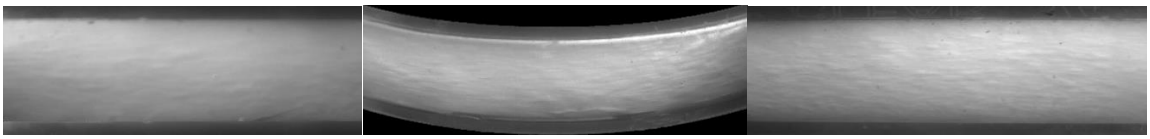

Figure 9: Camera images of dispersed water in oil flow at $U_{SO} = 0.27ms^{-1}$ and $U_{SW} = 0.96ms^{-1}$. From left to right: fully developed flow before the bend, at the bend and redeveloping flow after the bend

Flow pattern map: Figure 10 represents the flow pattern map upstream of (i.e. before) the bend superimposed on the flow pattern map at the bend. It should be noted that the flow pattern maps at the bend and redeveloping downstream of (i.e. after) the bend are very similar. Hence, the reason why flow pattern map of the redeveloping flow after the bend was not presented. The obvious difference between the flow pattern maps before and at the bend (or redeveloping downstream of the bend) was that Do/w/w persisted over a wider range of oil superficial velocity for the later. This observed flow pattern behavior is consistent with the report of Sharma et al. (2011b).

Preprints (www.preprints.org) | NOT PEER-REVIEWED | Posted: 16 May 2020 doi:10.20944/preprints202005.0278.v1

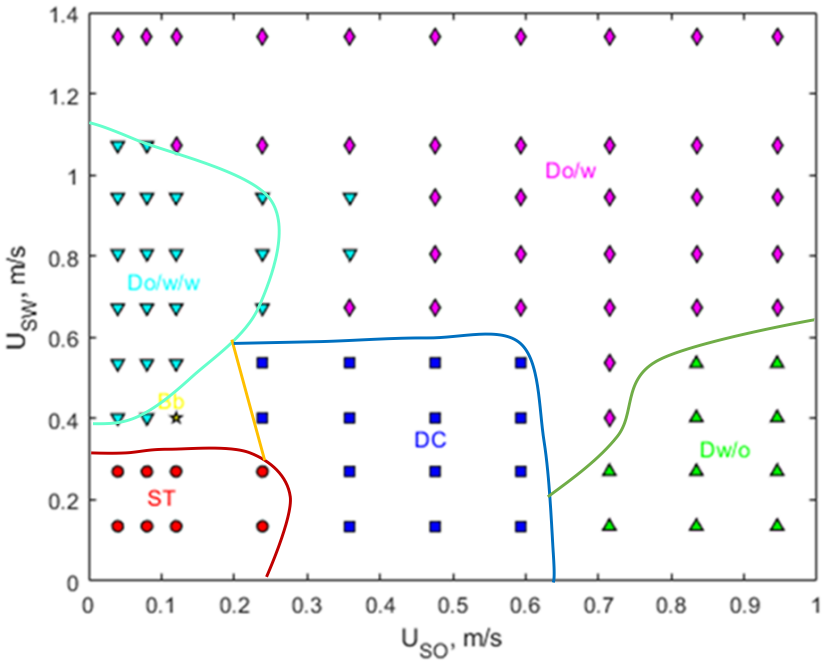

Figure 10: Flow pattern maps for before the bend (solid lines) and at the bend (symbols)

3.2 Pressure gradient for co-current oil and water flow in and around U-bend

In [1], [18], [27]

In specific terms, , plots of measured pressure gradient of co-current oil and water flow before -, at - and two redeveloping locations downstream of - the U-bend versus oil fraction at various water superficial velocities are presented. The general characteristics of the curves are similar in all test locations but they reveal an increase in pressure gradient with oil fraction. The later trend agrees with previous study on co-current oil and water flow in horizontal tubes [1], [18], [27]

In specific terms, [*1*], [18], [27]

In specific terms, a shows the pressure gradient versus oil fraction for oil-water flows in the fully developed flow section upstream of the bend. Over the measurement conditions considered in the present study, there were two distinct regions in the plots corresponding to separated flow and mixed flow regimes. Between these two flow regimes, there appeared to be a transition region (dash-curves in [*1*], [18], [27]

In specific terms, a), which was always found within the range of $0.4 \leq U_{sw} \leq 0.54\ m/s$. As oil and water velocities were increased, the flow pattern moved from separated flow to mixed flow. This behavior was also observed at the bend and downstream of the bend ([1], [18], [27]

In specific terms, b–d) albeit to different degrees. For example, the transition in [*1*], [18], [27]

In specific terms, c, as indicated by circled points, corresponds to a transition from dual continuous flow (separated flow) to dispersed flow (mixed flow) downstream of the bend. In the DC flow, the mixing was restricted to a region close to the interface and droplets of either phases were observed in the other phase [1], [28]. At transition, as in this case, there was significant mixing in the entire oil layer and water bubbles were observed close to the top section of the pipe. It was also observed that the continuous oil layer at the top-half of the pipe began to break up resulting in an oscillating flow behavior. This resulted in a significant

Preprints (www.preprints.org) | NOT PEER-REVIEWED | Posted: 16 May 2020 doi:10.20944/preprints202005.0278.v1

decrease in time averaged pressure gradient because the contribution of the more viscous phase (oil) to wall frictional losses reduced.

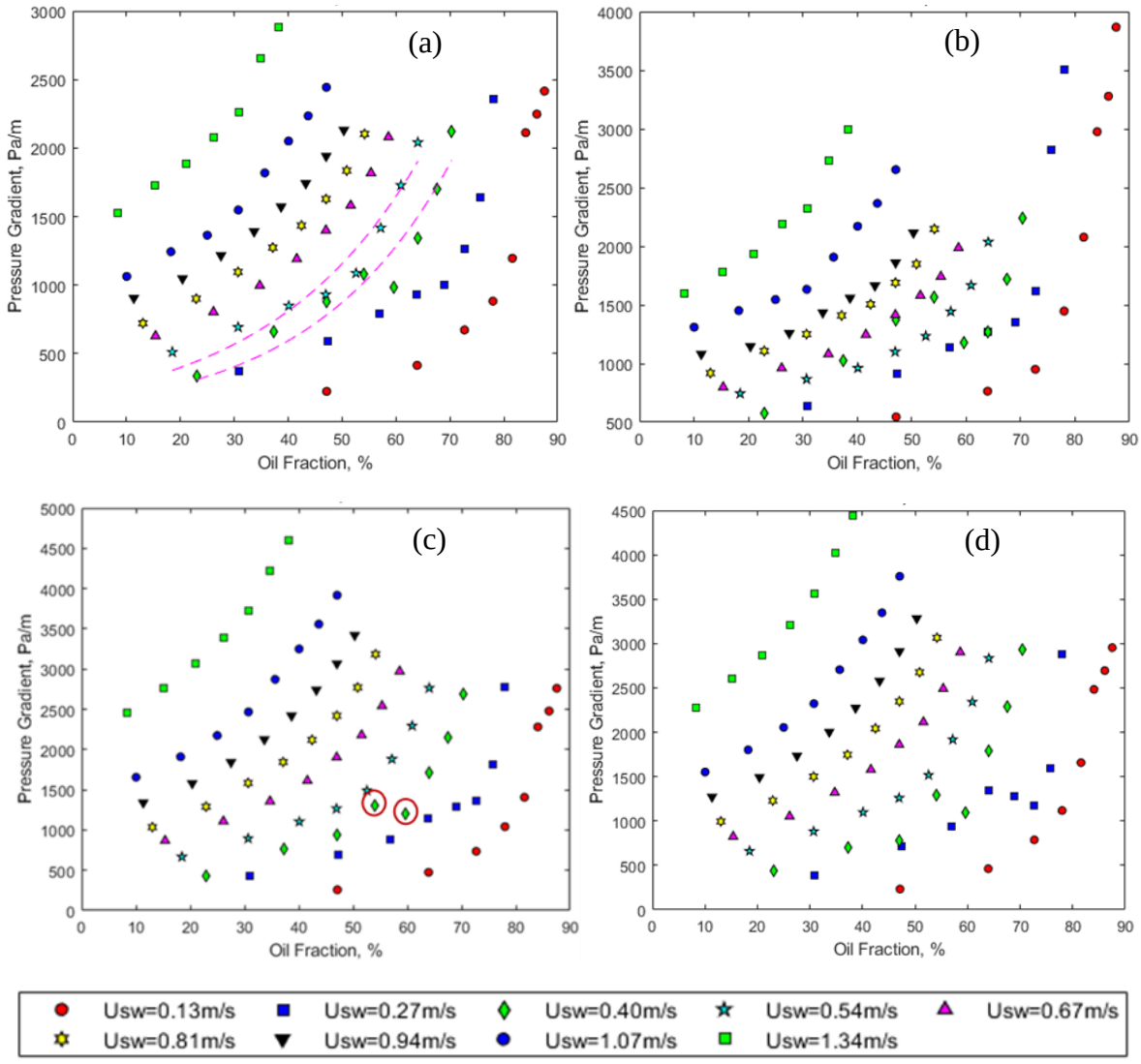

Figure 11: Pressure gradient variation with oil fraction at different water superficial velocities. (a) before the bend, (b) at the bend, (c) location 1 after the bend, (d) location 2 after the bend.

To compare the pressure gradient at the various test locations in and around the U-bend, plots of pressure gradient versus oil fraction at selected water superficial velocities are provided in Figure *12*. At low water superficial velocity of 0.13 m/s (Figure *12*a), pressure gradient curves before and after the bend collapsed into a single curve especially at low oil fraction the pressure while that at the bend was noticeably higher than those upstream and downstream of the bend at lower oil fractions. This is because at low mixture velocities, the contribution of secondary flows to pressure drops relative to those of wall and interfacial frictions is significant. In addition, pressure gradient curves for all the test locations at this flow condition also showed a moderate increase at low oil fractions and an exponential increase with high oil fractions. This was due to the increase in the mixture viscosity as the oil fraction increased. With increase in the flowrate of water, the pressure drops showed different trends in all test locations and at various oil fractions (Figure *12*b). At lower oil fraction (and lower mixture velocity), pressure gradient at the bend was expectedly higher than those before and after the bend. At higher

Preprints (www.preprints.org) | NOT PEER-REVIEWED | Posted: 16 May 2020 doi:10.20944/preprints202005.0278.v1

mixture velocity, where turbulence dominated, the pressure gradients at the bend and those before the bend converged. Interestingly, at higher mixture velocity/oil fraction, the pressure gradients for the two redeveloping locations after the bend were higher than those before the bend and at the bend. This is because flow disturbances after the bend became significant and the contribution of form drag to pressure losses was quite significant at these high mixture velocities. At even higher mixture velocities (Figure *12*c and 2d), this trend of the pressure gradients became even much more pronounced. At such high Reynolds number (Figure 12d), pressure drop after the bend corresponded to over 60% of the total pressure drop in the combined test section (measurement from Foxboro DP cell for combined section). The difference between these two figures is that the pressure gradients at the bend were higher than those before the bend at low oil fractions but they both converged at high oil fractions in Figure *12*c. This is attributed to the wall and interfacial effect that dominated in Figure 12d and therefore both pressure gradient curves showed similar characteristics irrespective of oil fraction.

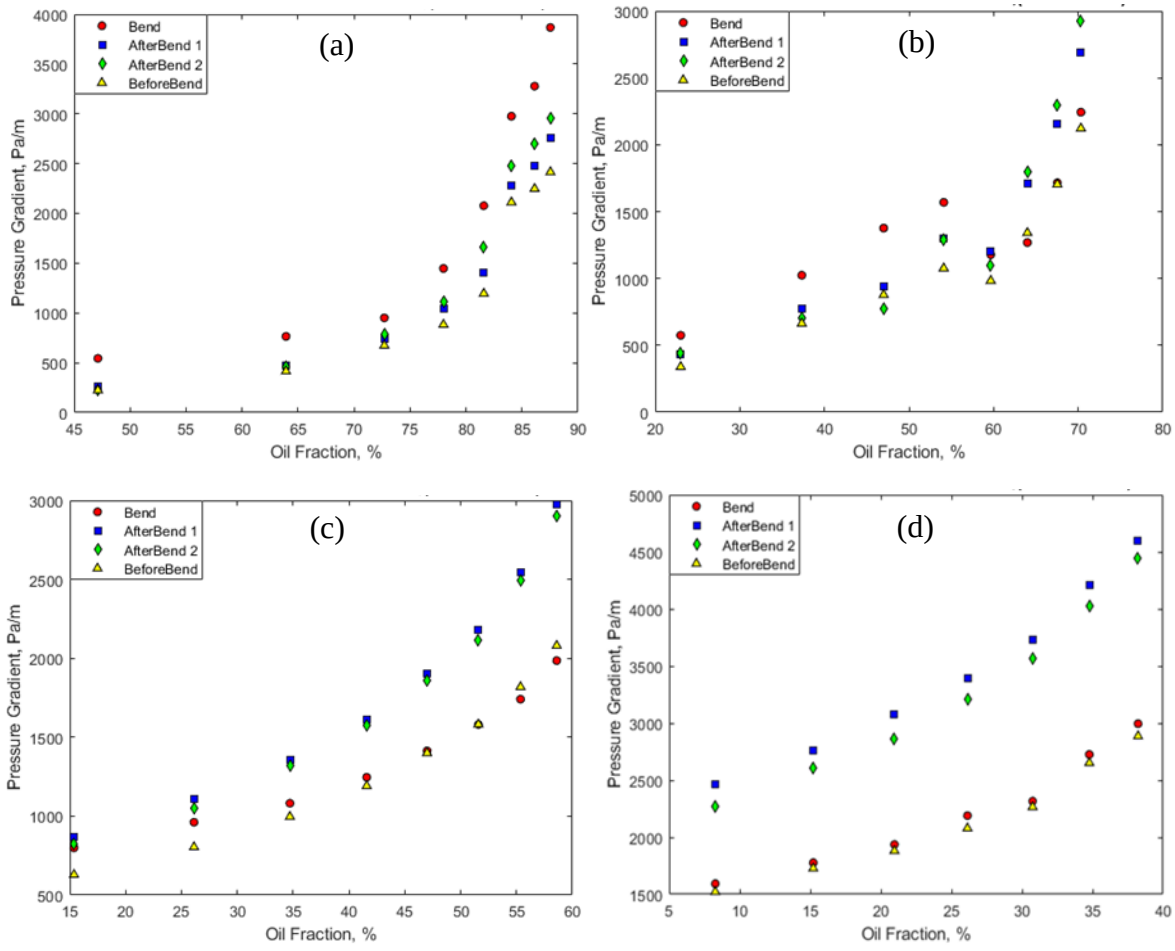

Figure 12: Comparison of pressure gradients in and around U-bend for oil-water flows at selected water superficial velocities. (a) $U_{SW} = 0.13\ m/s$, (b) $U_{SW} = 0.40\ m/s$, (c) $U_{SW} = 0.67\ m/s$, (d) $U_{SW} = 1.34\ m/s$.

Results of pressure gradients versus water superficial velocities are also presented to highlight the effect of changes in U_{SW} on pressure gradient in and around bends (Figure *13*). At low U_{SW}, the pressure gradient in the bend superseded those before the bend due to the significant

Preprints (www.preprints.org) | NOT PEER-REVIEWED | Posted: 16 May 2020 doi:10.20944/preprints202005.0278.v1

contribution of secondary flows to pressure drops relative to turbulence (Figure *13*a). At higher water superficial velocities, a larger percentage of pressure drops occurred at the redeveloping sections after the bend. In addition, the pressure gradients immediately after the bend were slightly higher than those further downstream of the bend. This suggest that the contribution of form drag to pressure drops is a function of the level of flow redevelopment. Interestingly, the trajectory of the curves for both redeveloping locations after the bend are similar and this suggests that similar forces were at play in both redeveloping locations. Figure 13a also highlights the region of flow transition ($0.4 \leq U_{sw} \leq 0.54\ m/s$) discussed earlier. In the water dominant regime, increase in U_{SW} resulted in increase in the difference between the pressure gradients in the redeveloping flows and those before and at the bend. At significantly high oil superficial velocity (Figure *13*b), the characteristics of the curves are somewhat different and the transition velocities depended on the test location. For instance, at $U_{SW} < 0.54$ m/s where the oil phase dominated, the pressure gradients generally decreased with increase in U_{SW}, and water acted as a drag reducing agent. As the mixture velocity was increased further, minimum pressure gradients were attained after which further increase in flowrate resulted in higher pressure gradients. At these high mixture velocities, the mixture Reynolds numbers, which was responsible for the turbulence intensity, largely determined the pressure gradients. These results are generally consistent with reports of Yusuf et al., (2012), [1], [29] and Al-Wahaibi et al. (2014) (straight pipe) and Sharma et al., (2011b, 2011a) (U-bend) within comparable oil-superficial velocity range.

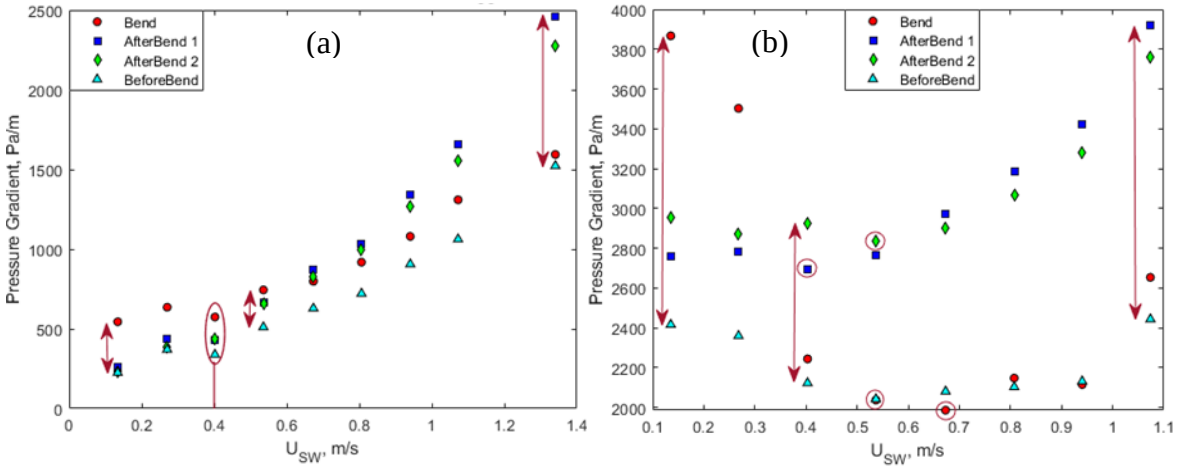

Figure 13: Comparison of the pressure gradients in and around U-bends for oil-water flows at selected U_{SO}. (a) $U_{SO} = 0.12\ m/s$, (b) $U_{SO} = 0.96\ m/s$

4 CONCLUSION

Experimental measurements of the flow patterns and pressure drops for oil-water flow in and around U-bend were carried out with the view of investigating the effect of the bend on oil-water flow characteristics. Based on results obtained, the following conclusion could be drawn.

- Flow patterns in the various test locations were largely similar. However, the transition mixture velocity of the flow before the bend sometimes different from those at the bend and after the bend.

- Pressure gradients at all the test locations increased with both oil fraction and water superficial velocity and there was a change of pressure gradient profile at the point of inversion from oil dominant to water dominant flow regime.
- Pressure gradients differed with respect to test location and the difference was strongly related to the superficial velocity of the phases and the flow pattern. In general, at high mixture velocity, pressure gradients at the redeveloping flow after the bend were higher than those before the bend and those at the bend. At low mixture velocity, pressure gradients at the bend were higher than those before and those after the bend.
- Pressure gradients immediately after the bend were generally higher than those further downstream after the bend. This indicates that there was decrease in pressure drops with level of flow development downstream of the bend.

ACKNOWLEDGEMENT

The Authors would also like to acknowledge the United States J.W. Fulbright Program/U.S. Department of State and Institute of International Education (IIE) for the funding provided for this research. The authors also wish to thank the Flow Group of University of California Berkeley and in particular Simo A. Mäkiharju, Eric Thacher and Daniel Grieb for the support provided for this research. The authors also wish to acknowledge the free donation of HPAM polymer for this research by BASF-Chemicals USA.

CONFLICT OF INTEREST.

The Authors wish to declare that there are no conflicts of interest with the publication of this manuscript.

REFERENCES

[1] L. C. Edomwonyi-Otu and P. Angeli, “Pressure drop and holdup predictions in horizontal oil-water flows for curved and wavy interfaces,” *Chem. Eng. Res. Des.*, vol. 93, pp. 55–65, 2015.

[2] M. M. Mandal, P. Aggarwal, and K. D. P. Nigam, “Liquid-liquid mixing in coiled flow inverter,” *Ind. Eng. Chem. Res.*, vol. 50, no. 23, pp. 13230–13235, 2011.

[3] P. O. Ayegba, M. Abdulkadir, V. Hernandez-Perez, I. S. Lowndes, and B. J. Azzopardi, “Applications of artificial neural network (ANN) method for performance prediction of the effect of a vertical 90° bend on an air–silicone oil flow,” *J. Taiwan Inst. Chem. Eng.*, vol. 0, pp. 1–6, 2017.

[4] P. O. Ayegba and M. Abdulkadir, “Prediction of Average Void Fraction and Pdf of Void Fraction in Vertical 90 O Bend for Air–Silicone Oil Flow Using Multilayer Perceptron (Mlp) Codes,” *Int. J. Lean Think.*, vol. 7, no. 2, pp. 80–105, 2016.

[5] S. Ghosh, T. K. Mandal, G. Das, and P. K. Das, “Review of oil water core annular flow,” *Renew. Sustain. Energy Rev.*, vol. 13, no. 8, pp. 1957–1965, 2009.

[6] D. Strazza and P. Poesio, “Experimental study on the restart of core-annular flow,” *Chem. Eng. Res. Des.*, vol. 90, no. 11, pp. 1711–1718, 2012.

[7] S. Tripathi, A. Bhattacharya, R. Singh, and R. F. Tabor, “Lubricated Transport of Highly Viscous Non-Newtonian Fluid as Core-annular Flow: A CFD Study,” *Procedia IUTAM*, vol. 15, pp. 278–285, 2015.

[8] W. L. Loh and V. K. Premanadhan, "Experimental investigation of viscous oil-water flows in pipeline," *J. Pet. Sci. Eng.*, vol. 147, pp. 87–97, 2016.

[9] M. Ameri and N. Tirandaz, "Two phase flow in a wavy core-annular configuration through a vertical pipe: Analytical model for pressure drop in upward flow," *Int. J. Mech. Sci.*, vol. 126, no. February, pp. 151–160, 2017.

[10] A. Goldstein, A. Ullmann, and N. Brauner, "Exact solutions of core-annular laminar inclined flows," *Int. J. Multiph. Flow*, vol. 93, pp. 178–204, 2017.

[11] E. van Duin, R. Henkes, and G. Ooms, "Influence of oil viscosity on oil-water core-annular flow through a horizontal pipe," *Petroleum*, pp. 1–7, 2018.

[12] Y. Zhou, S. N. Shah, and P. V Gujar, "Effects of coiled-tubing curvature on drag reduction of polymeric fluids," *SPE Prod. Oper.*, vol. 21, no. 1, pp. 134–141, 2004.

[13] K. Gasljevic and E. F. Matthys, "Friction and heat transfer in drag-reducing surfactant solution flow through curved pipes and elbows," *Eur. J. Mech. / B Fluids*, vol. 28, no. 5, pp. 641–650, 2009.

[14] P. O. Ayegba, L. C. Edomwonyi-Otu, N. Yusuf, and A. Abubakar, "Results in Materials Experimental and neural network modelling of polymer drag reduction in 180 bends," *Results Mater.*, vol. 1, pp. 1–11, 2019.

[15] P. O. Ayegba and L. C. Edomwonyi-Otu, "Turbulence statistics and flow structure in fluid flow using PIV technique: A review," *Eng. Reports*, no. August 2019, pp. 1–49, 2020.

[16] N. Yusuf, Y. Al-Wahaibi, T. Al-Wahaibi, A. Al-Ajmi, A. S. Olawale, and I. A. Mohammed, "Effect of oil viscosity on the flow structure and pressure gradient in horizontal oil – water flow," *Chem. Eng. Res. Des.*, vol. 90, no. 8, pp. 1019–1030, 2012.

[17] L. C. Edomwonyi-Otu and P. Angeli, "Separated oil-water flows with drag reducing polymers," *Exp. Therm. Fluid Sci.*, vol. 102, no. September 2017, pp. 467–478, 2019.

[18] T. Al-Wahaibi, Y. Al-Wahaibi, A. Al-Ajmi, R. Al-Hajri, N. Yusuf, and A. S. Olawale, "Experimental investigation on fl ow patterns and pressure gradient through two pipe diameters in horizontal oil – water flows," *J. Pet. Sci. Eng.*, vol. 122, pp. 266–273, 2014.

[19] A. I. Dosumu, L. C. Edomwonyi-Otu, N. Yusuf, and A. Abubakar, "Guar Gum as Flow Improver in Single-Phase Water and Liquid–Liquid Flows," *Arab. J. Sci. Eng.*, 2020.

[20] M. N. Abdallah, L. C. Edomwonyi-Otu, N. Yusuf, and A. Baba, "Aloe Vera Mucilage as Drag Reducing Agent in Oil-Water Flows," *Arid Zo. J. Eng. Technol. Environ.*, vol. 15, no. 2, pp. 248–258, 2019.

[21] M. Pietrzak, "Flow patterns and volume fractions of phases during liquid – liquid two-phase flow in pipe bends," *Exp. Therm. Fluid Sci.*, vol. 54, pp. 247–258, 2014.

[22] M. Sharma, P. Ravi, S. Ghosh, G. Das, and P. K. Das, "Hydrodynamics of lube oil – water flow through 180o return bends," *Chem. Eng. Sci.*, vol. 66, no. 20, pp. 4468–4476, 2011.

[23] M. Sharma, P. Ravi, S. Ghosh, G. Das, and P. K. Das, "Studies on low viscous oil-water flow through return bends," *Exp. Therm. Fluid Sci.*, vol. 35, no. 3, pp. 455–469, 2011.

[24] P. Angeli and G. F. Hewitt, "Flow structure in horizontal oil-water flow," *Int. J. Multiph. Flow*, vol. 26, no. 7, pp. 1117–1140, 2000.

[25] S. Ghosh, G. Das, and P. Kumar, "Simulation of core annular in return bends — A comprehensive CFD study," *Chem. Eng. Res. Des.*, vol. 89, no. 11, pp. 2244–2253, 2011.

[26] M. Al-Yaari, A. Al-Sarkhi, and B. Abu-Sharkh, "Effect of drag reducing polymers on water holdup in an oil-water horizontal flow," *Int. J. Multiph. Flow*, vol. 44, pp. 29–33, 2012.

[27] L. C. Edomwonyi-Otu, M. Chinaud, and P. Angeli, "Effect of drag reducing polymer on horizontal liquid-liquid flows," *Exp. Therm. Fluid Sci.*, vol. 64, pp. 164–174, 2015.

[28] L. C. Edomwonyi-Otu, A. H. Barral, and P. Angeli, "Oil-Water flow characteristics in pipes of different diameters," *Niger. J. Mater. Sci. Eng.*, vol. 5, no. 1, pp. 35–40, 2014.

[29] L. C. Edomwonyi-Otu, A. H. Barral, and P. Angeli, "Influence of Drag Reducing Agents on Interfacial Wave Characteristics in Horizontal Oil-Water Flows," in *The 16th International Conference on Multiphase Production Technology*, 2013, pp. 353–362.